Apparent Directional Scanning for DNA Repair

Tong Zhao and Aaron R. Dinner
Department of Chemistry, James Franck Institute, and Institute for Biophysical Dynamics, The University of Chicago, Chicago, Illinois

ABSTRACT Recently it was observed that the DNA repair protein human O^6-alkylguanine-DNA alkyltransferase repairs lesions at the 5′ ends of 70-nucleotide single-stranded DNA roughly threefold more frequently than lesions at the 3′ ends. Here, we introduce a coarse-grained model to show how a local asymmetry in binding kinetics (rather than thermodynamics) together with irreversible alkyl transfer can give rise to this apparent bias in sequence scanning. Exploration of the parameter space provides quantitative relationships that can be used to validate the proposed mechanism by gel-based assays.

INTRODUCTION

To perform their functions efficiently, site-specific DNA-binding proteins must locate their targets among millions of basepairs. Seminal work in the 1970s and 1980s showed that the *Escherichia coli* lac repressor could accelerate binding to its operator site on λ-DNA in vitro by as much as 1000-fold relative to a random walk in solution by ''facilitated diffusion'' (1,2). The essential idea is that nonspecific binding dramatically increases the effective size of the target (the whole DNA molecule) and decreases that of the search space (one dimension, instead of three) (3). Specific elaborations of this basic mechanism for efficient exploration of the sequence and its readout invoke sliding, hopping, intersegmental transfer, and conformational changes of both the protein and the DNA (4–8).

Facilitated diffusion is expected to be directionally unbiased because it does not consume cellular energy sources (e.g., by hydrolyzing ATP), in contrast to the movement of molecular motors (9,10). Strikingly, Tainer and co-workers recently observed apparent 3′–5′ scanning for the human DNA repair protein O^6-alkylguanine DNA alkyltransferase (AGT) (11). In the experiments, O^6-methylguanine lesions near the 5′ end of a 70-nucleotide single-stranded (ss) DNA oligomer were repaired 3.3 ± 0.9 times faster than those near the 3′ end. The preference was abolished by introducing a biotin-streptavidin block to AGT binding at position 23 of the DNA. This observation, together with the fact that the lesions were located in the middle of identical 11-nucleotide sequences, suggests that the preference for the 5′ substrates is not simply a sequence-dependent end-binding effect on affinity. Functionally, such 3′–5′ directed scanning could enhance the efficiency of lesion detection in a genomic context by enabling AGT to clean the template strand immediately before the DNA was read by RNA polymerase (12).

In this article, we introduce a mathematical model that shows how a bias in repair can arise in this system. Motivated by equilibrium measurements (13,14), we explore the consequences of the idea that a protein molecule already on the DNA influences the kinetics (rather than the thermodynamics) of additional copies binding on its 5′ and 3′ sides differently. The model shows that the relative frequency of repair at the 5′ and 3′ lesions varies with important physical characteristics of the system (their separation, protein concentrations, position and size of the block, and kinetic parameters). The predicted scaling relationships provide a quantitative means of experimentally testing the qualitative mechanism.

METHODS

Our goal is to show how biased repair can arise without directly using cellular energy sources. Equilibrium measurements show that multiple copies of AGT bind ssDNA (13,14). An important additional feature of AGT is that it repairs lesions by irreversibly transferring alkyl groups to an active site cysteine. We use a discrete master equation to show that this feature, combined with a binding scheme in which copies of the protein bind and unbind more quickly on the 5′ sides than the 3′ sides of copies already on the DNA (e.g., due to distortion of the DNA structure by the molecule already bound), gives rise to apparent directional scanning.

For mathematical simplicity, we treat the DNA as a one-dimensional lattice and assume the solution is sufficiently well mixed that we can treat binding as unimolecular with rate constant ν_0. This mean-field approximation does not impact the results significantly because nonspecific encounters between protein and DNA molecules cannot produce a 5′–3′ bias in net repair rates even if one accounts for fluctuations. The unbinding rate is $\gamma\nu_0$, where the dimensionless ratio γ can be viewed as the effective equilibrium constant for a site in the absence of binding cooperativity and is assumed to be sequence independent. Equilibrium measurements indicate that multiple AGTs bind with significant cooperativity to ssDNA (13,14), so we augment the basic thermodynamics with a nearest-neighbor interaction between bound proteins on the lattice. We incorporate this interaction into the unbinding rate: $\gamma\nu_0 \rightarrow \omega^{-n}\gamma\nu_0$ where $n = 0$, 1, or 2 is the number of nearest neighbors. The cooperativity parameter, ω, is defined to be the equilibrium constant for the process of moving a protein from an isolated site to a singly contiguous one or from a singly contiguous site to a doubly contiguous one (14).

It is important to note that equilibrium binding cooperativity by itself is insufficient to produce the bias in repair rate because the nearest-neighbor interactions are symmetric (Fig. 1 *A*). For preferential repair without

Submitted April 11, 2007, and accepted for publication August 15, 2007.

Address reprint requests to Aaron R. Dinner, Gordon Center for Integrative Science, 929 East 57th St., Chicago, IL 60637. Tel.: 773-702-2330; Fax: 773-834-5250; E-mail: dinner@uchicago.edu.

Editor: Tamar Schlick.

0006-3495/08/01/47/06 $2.00

doi: 10.1529/biophysj.107.110619

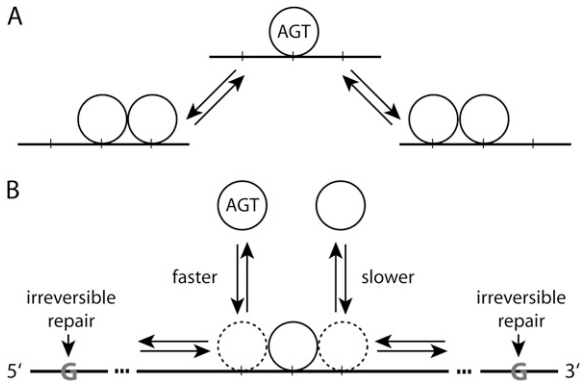

FIGURE 1 Schematics of the model. The DNA is represented by a one-dimensional lattice and the proteins are drawn as circles (not to scale with the lattice spacing). (*A*) Equilibrium binding cooperativity cannot give rise to a directional bias in the net repair rate because the two lower configurations have the same free energies. (*B*) Summary of asymmetric kinetics.

violation of the second law of thermodynamics, the mechanism must also depend on the path for forming a repair-competent protein-DNA configuration and thus be kinetic in nature. In particular, we consider the case that binding is accelerated (decelerated) when a protein copy is already bound on the 3′ (5′) side of a site of interest (Fig. 1 *B*). To this end, we introduce dimensionless parameters $\Delta_{\pm}$ to characterize rate enhancements relative to the basic rate: $\nu_0 \rightarrow \nu_0\Delta_{\pm}$ with $\Delta_+ > 1$ and $\Delta_- < 1$. The binding rate when both sides are occupied is ν_1, which we treat as an additional free parameter (i.e., ν_1 need not equal $\nu_0\Delta_+\Delta_-$). Denoting the probability of occupancy at site i by p_i, the binding rate is thus

$$\begin{aligned}\nu_+(p_{i-1},p_{i+1}) &= \nu_0(1-p_{i-1})(1-p_{i+1})\\ &\quad+\nu_0\Delta_+(1-p_{i-1})p_{i+1}+\nu_0\Delta_-p_{i-1}(1-p_{i+1})\\ &\quad+\nu_1p_{i-1}p_{i+1}. \qquad (1)\end{aligned}$$

The unbinding rate can be written in terms of the dimensionless equilibrium constants defined previously:

$$\begin{aligned}\nu_-(p_{i-1},p_{i+1}) &= \gamma\nu_0(1-p_{i-1})(1-p_{i+1})\\ &\quad+\omega^{-1}\gamma\nu_0[\Delta_+(1-p_{i-1})p_{i+1}\\ &\quad+\Delta_-p_{i-1}(1-p_{i+1})]+\omega^{-2}\gamma\nu_1p_{i-1}p_{i+1}. \qquad (2)\end{aligned}$$

In addition to binding and unbinding, we assume that the protein at site i can move to an adjacent unoccupied site ($j = i \pm 1$) along the DNA by either sliding or hopping locally with rate Γ_i. Accounting for the nearest-neighbor interactions, Γ_i is given by

$$\begin{aligned}\Gamma_i &= \Gamma_0(1-p_{i-1})(1-p_{i+1})\\ &\quad+\omega^{-1}\Gamma_0[p_{i-1}(1-p_{i+1})+p_{i+1}(1-p_{i-1})], \qquad (3)\end{aligned}$$

where Γ_0 is the hopping rate for a single protein on DNA. The dynamics can then be summarized in the master equation

$$\begin{aligned}\frac{dp_i}{dt} &= \frac{\Gamma_i}{2}(p_{i-1}-p_i)+\frac{\Gamma_i}{2}(p_{i+1}-p_i)\\ &\quad+\nu_+(p_{i-1},p_{i+1})(1-p_i)-\nu_-p_i. \qquad (4)\end{aligned}$$

For simplicity, here we neglect processes that depend on transfer of the protein from one part of the DNA to another through three-dimensional space. Incorporating such effects does not change the qualitative conclusions, as discussed in the Results and Discussion section.

We solve Eqs. 1–4 with a continuous time Monte Carlo algorithm (15–17). Each simulation starts with an empty DNA lattice. At each step, all possible transitions which can be reached in one Monte Carlo step from the current state are determined. Proteins can bind to any unoccupied site along the DNA, and the bound proteins can unbind from any occupied site with rates determined by their local environments, as defined through Eqs. 1 and 2. Hopping is allowed subject to a variable rate according to Eq. 3. The new state is chosen stochastically with probability proportional to the respective transition rate. The time increment is inversely proportional to the total extent of reaction measured by the sum of all the rates (k_{tot}), $\Delta t = -\ln r/k_{tot}$, where r is a random number uniformly distributed in [0, 1). The simulation is terminated when a protein binds or hops to either lesion site.

We work in natural units of length and time for the system: $a = 0.34$ nm (a typical nucleotide separation) and $\tau = 1$ μs. In these units, we estimate the parameters as follows.

Γ_0: Single molecule experiments measure the diffusion constant of human oxoguanine DNA glycosylase 1 (hOgg1) along double-stranded (ds) DNA stretched by shear flow to be $D_{1d} = 5 \times 10^6$ bp^{2}s^{-1}, and that measured for the C-terminal domain of Ada, a bacterial homolog of AGT, is comparable (Y. Lin, T. Zhao, Z. Farooqui, X. Qu, C. He, A. R. Dinner, and N. F. Scherer, unpublished data). In the absence of data for AGT on ssDNA, we choose a hopping rate of $\Gamma_0 = 2D_{1d}/a^2 = 2/\tau$ (which corresponds to $D = 10^6$nt^{2}s^{-1}) for this study.

ν_0: The nonspecific bare binding rate depends on the encounter probabilities of the protein and DNA, which can be estimated from the classic Smolouchowski limit (2). Using this approach, we expect the diffusion limited binding rate for the AGT-ssDNA system to be in the range 10^2–10^5 s^{-1}. We choose $\nu_0 = 0.001/\tau = 10^3$ s^{-1}.

γ: The dimensionless equilibrium constant γ is closely related to the escape probability P of a single protein. As discussed in a number of previous studies (see Halford and Marko (7)), P is expected to be small since the dissociation from a nonspecific binding site requires the protein to achieve a separation of ~1 nm from the DNA to escape the counterion atmosphere. An order of magnitude estimate can be obtained from D_{1d} and the lifetime on the DNA (τ_{DNA}) (18). Defining $l \sim D_{1d}\tau_{DNA}/a^2$, $(1-P)^l \sim 1 - lP = 0$ or $P = 1/l \sim 10^{-6}$–10^{-4} per site. A protein can either slide along the DNA or hop off it, so the escape probability is $P \simeq \gamma\nu_0/(\gamma\nu_0+\Gamma_0)$; thus we have $\gamma \sim 0.01$–1. In the simulations presented, we take $\gamma = 0.1$ unless otherwise specified.

ω: For ssDNA ranging from 5 to 78 nt, the cooperativity parameter ω is estimated to be between 37.9 ± 3.0 and 89.8 ± 8.9 (14). Here, we employ a value of $\omega = 65$.

Enhancement factors: The dimensionless enhancement and reduction factors $\Delta_{\pm}$ are not experimentally measured, and we estimate them by comparing the simulations with the measured repair rates. The binding rate with both neighbors present (ν_1) is in principle a free parameter, but for simplicity we always set it to be $\nu_0 \min(\Delta_+, \Delta_-)$. As shown in the next section, varying ν_1 has virtually no effect on our results.

It is important to note that the measurements for the diffusion constant (18) require a certain degree of interpretation to apply them to the ssDNA case of interest here (19). Furthermore, we neglect the length dependence observed for binding (14). The predicted trends are not sensitive to these details, as discussed further below.

RESULTS AND DISCUSSION

In this section, we use the Monte Carlo method outlined above to determine the consequences of asymmetrically facilitated binding. The dynamics in the absence and presence of a biotin-streptavidin block are considered and compared with existing experimental observations to estimate the required binding rate enhancement factors. We also explore how the

ratio of 5′:3′ repair rates depends on various physical characteristics of the system.

Enhancement factors

We first apply the model to a one-dimensional lattice composed of 70 sites with lesions located symmetrically at a distance $5a$ from the system termini. We perform 1000 independent simulations and count the number of times the protein arrives at each lesion, which we denote $n_{5'}$ ($n_{3'}$) for the lesion near the 5′ (3′) end. Taking the repair to be diffusion limited (20), we can use the ratio $n_{5'}/n_{3'}$ as a surrogate for the actual ratio of repair rates. The consequences of this assumption and its relaxation are explored below. The dependence of the ratio of the occurrence numbers on the facilitated binding enhancement, which is characterized by the dimensionless parameter Δ_+, is shown in Fig. 2. As Δ_+ increases, the lesion near the 5′ end is preferentially repaired, as much as an order of magnitude more frequently. The system saturates for $\Delta_+ > 10^5$ due to the constraint of microscopic reversibility imposed by finite γ. Fig. 2 suggests that the experimentally observed ratio 3.3 ± 0.9 results from a 600-fold enhancement in binding rate.

Naively, one might suppose that a like bias could be achieved by making Δ_- small. However, this is not the case (data not shown). This asymmetry of the model can be understood by analogy with parallel resistors. For simplicity, let us assume $\Delta_+ = 1$ and $\Delta_- \ll 1$, so that binding on the 5′ side of an AGT molecule is much faster than on the 3′ side, as above. In this case, additional copies of the protein can still bind with rate ν_0 at sites not immediately 3′ to an AGT molecule already on the DNA. In other words, the path of high resistance can be circumvented. Thus preferential repair manifests only when binding is enhanced on at least one side of an AGT molecule already on the DNA.

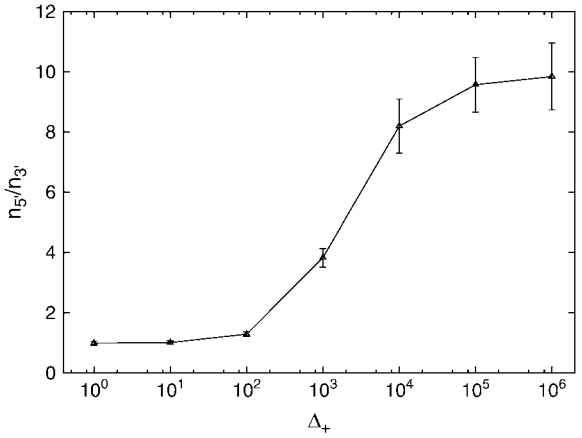

FIGURE 2 Dependence of bias on the factor by which the binding rate is enhanced on the 5′ sides of copies of AGT already on the DNA (Δ_+). The system size is $70a$, and the lesions are located at $6a$ and $65a$; $\Gamma_0 = 2/\tau$, $\nu_0 = \nu_1 = 0.001/\tau$, $\Delta_- = 1$, $\omega = 65$, and $\gamma = 0.1$.

DNA binding parameters

It is important to examine the dependence of the repair ratio on additional parameters in the model to identify experiments that can be used to validate the proposed mechanism. We begin with the bare binding rate ν_0, which characterizes the combined effects of diffusional encounter and protein concentration in the model. We find that the bias is small when there are few proteins on the DNA to facilitate the binding of additional copies (Fig. 3); the repair ratio saturates as ν_0 becomes large enough that nearly every lattice site is occupied. In contrast, the repair ratio does not depend significantly on ν_1 (Fig. 3) because inserting a protein when both its neighboring sites are already occupied does not enable relay of the binding enhancement.

Consistent with the fact that the DNA coverage influences the bias, the repair ratio decreases with γ, the dimensionless dissociation constant (Fig. 4). The propensity of the protein for the DNA can be manipulated experimentally by varying the concentration of the protein or salt in the solution. Low salt concentrations will promote binding and thus preferential repair, whereas high salt concentration will disfavor binding and lead to loss of the bias.

Although it is not readily experimentally manipulable, we also examined the dependence of the repair ratio on the cooperativity parameter ω by varying it from 1 to 150 (Fig. 5). Strengthening the nearest-neighbor interaction increases $n_{5'}/n_{3'}$ because it shifts the effective binding unit from a monomer to a multimer and thus increases the length scale over which the asymmetric binding operates.

DNA size effects

In addition to the kinetic and thermodynamic parameters, it is also of interest to investigate the dependence of the repair ratio on the system size. As discussed above, the thermodynamic

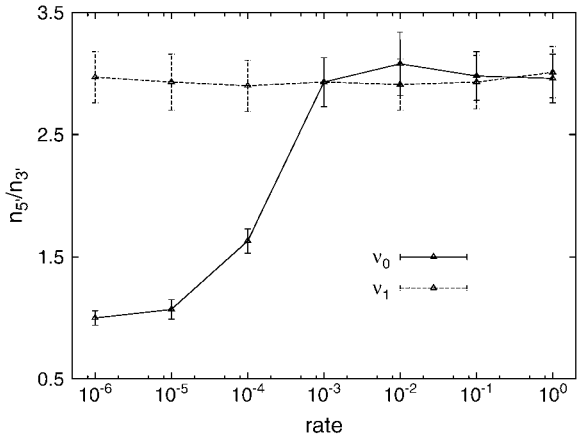

FIGURE 3 Dependence of the bias on the bare binding rate (ν_0, *solid line*) and the two-neighbor binding rate (ν_1, *dashed line*), both in units of $1/\tau$. Remaining parameters are the same as in Fig. 2 with $\Delta_+ = 600$.

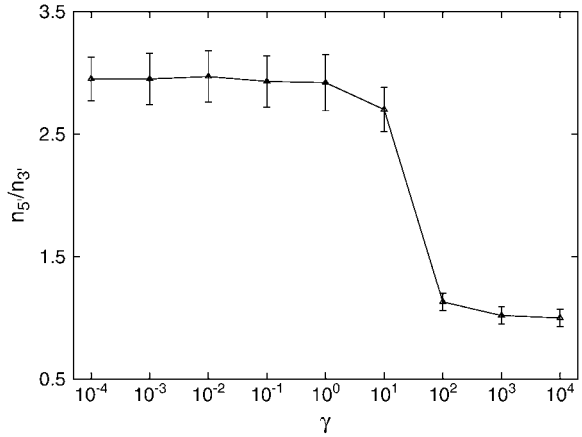

FIGURE 4 Dependence of the bias on the dimensionless dissociation constant. The system is otherwise the same as in Figs. 2 and 3.

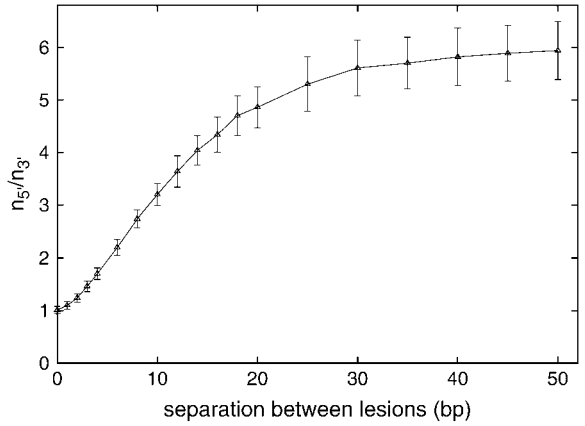

FIGURE 6 Dependence of the bias on the separation of the two lesions. The lesions are located at the ends of the lattice; otherwise the simulations are the same as in Figs. 2 and 3.

constraint of reversibility that we impose on the model puts bounds on the repair ratio. In particular, unbinding of interior proteins from a contiguous stretch of AGT molecules on the DNA causes the enhancement to have a persistence length. To estimate this length scale, we place the lesions at the ends of a finite one-dimensional lattice and vary their separation. We find the repair ratio begins to saturate at $\sim 15a$ (Fig. 6). Including a length dependence for ν_0 (14) would convolute the effects observed in Figs. 3 and 6 and accelerate the saturation.

It is important to note that the persistence length is expressed in units of lattice spacings (a). We can thus rescale the system without qualitatively changing the predictions above. Specifically, we can account for the size of an AGT molecule. If each AGT occupies ~ 5 nt (11,14), a 70-nt ssDNA corresponds to a lattice of ~ 14 sites, not 70, as above. However, the bias is essentially unaltered by this rescaling because the elemental rates also depend on a. Indeed, simulation of a 14-site system with $\Gamma' = \Gamma_0$, $\nu_0' = \nu_0/5$, $\nu_1' = \nu_1/5$ and $\Delta_+' = \Delta_+ = 600$ recapitulates the results for the 70-site system above (2.82 ± 0.18 compared with 2.93 ± 0.21).

Relative rate of diffusion

In Fig. 7, we explore the dependence of the repair ratio on the hopping rate. Because hopping acts to randomize the protein distribution, it disfavors the bias. Preferential repair is abolished when Γ_0 is comparable to the enhanced binding rate $\nu_0\Delta_+$. As mentioned above, we explicitly consider only local hopping along the DNA. Transfer of the protein from one segment of the DNA to another through three-dimensional space (''intersegmental transfer'' or ''macroscopic hopping'' (2,7,8)) can provide a second channel for unbiased movement and thus is qualitatively equivalent to an increase in Γ_0. Similarly, we can relax the assumption that the reaction is diffusion controlled by incorporating catalysis

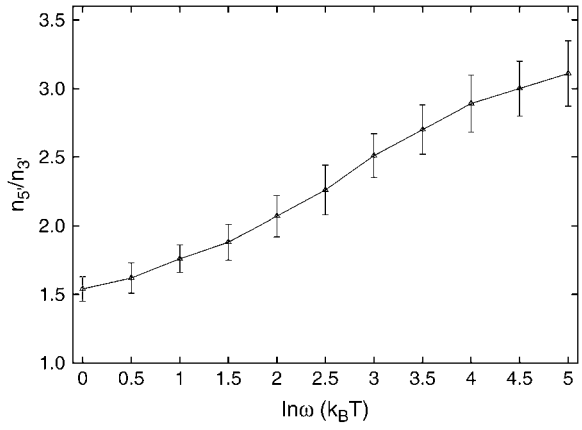

FIGURE 5 Dependence of the bias on the cooperativity parameter. The system is otherwise the same as in Figs. 2 and 3.

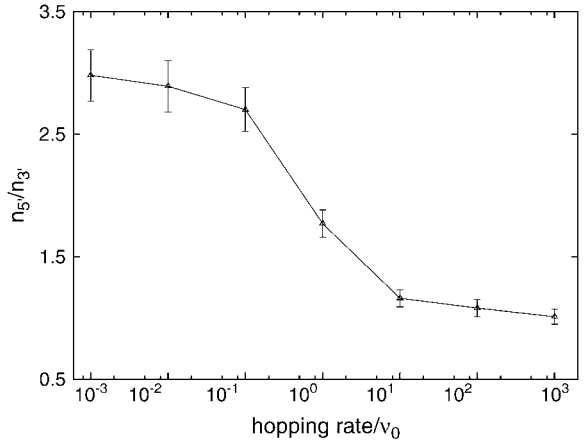

FIGURE 7 Dependence of the bias on the hopping rate (relative to the bare binding rate, Γ_0/ν_0). The system is otherwise the same as in Figs. 2 and 3.

explicitly into the stochastic simulations. The bias decreases as repair becomes slower (Fig. 8). We thus predict that catalytically compromised mutants of AGT will exhibit less bias in repair than the wild-type.

Biotin-streptavidin block

Introduction of a biotin-streptavidin group on the DNA hinders AGT binding by preventing access to sites in both a dynamic sense and a static one. The effective size of the block depends on the configuration of the DNA-biotin-streptavidin complex. For the block to impact the repair ratio, it must be sufficiently large that it is within the aforementioned persistence length of the lesions (Fig. 6). To demonstrate this relation explicitly, we model the block as a segment of sites to which the protein cannot bind. As shown in Fig. 9, the bias progressively decreases with the block size and disappears at 50 nt, the point at which each lesion is surrounded by exactly five sites on either of its sides. By the same token, if the block is shifted off the center of the DNA in the 3′ (5′) direction, the bias is amplified (diminished) (Fig. 10). In the experiments described in the Introduction (11), the block is located off center, at 23 nt from the 5′ end. To estimate the effective size of the block, we varied the number of excluded sites on a 70*a* lattice with the center of the excluded region at 23*a*. A repair ratio equal to that observed (1.0 ± 0.1) was obtained for a block size of 20*a*. Although this number appears large, it is in fact quite reasonable given the sizes of biotin and streptavidin.

CONCLUSIONS

In this article, we quantitatively explored a novel mechanism of facilitated diffusion motivated by recent experiments (11,14). The key idea is that the protein combines irreversible alkyl transfer with a cooperative binding scheme in which copies of the protein bind and unbind more quickly on the 5′ sides than the 3′ sides of copies already on the DNA. The apparent directional scanning that results is a kinetic, not a thermodynamic, effect. Stochastic master equation simulations of the model reproduce the existing experimental findings, and the 5′ enhancement factor is estimated to be roughly 600-fold. Our studies of the dependence of the bias on experimentally manipulable parameters (protein and salt concentrations, sequence length, block size and position) provides the first predictions that can be used to validate the mechanism by bulk solution phase assays. Nevertheless, single-molecule experiments analogous to those for hOgg1 (18) would be of interest because the molecular basis for the spatially local binding rate enhancement could be probed.

In assessing whether preferential repair significantly impacts repair function in vivo, it is important to keep in mind that the bias increases with the sequence length over

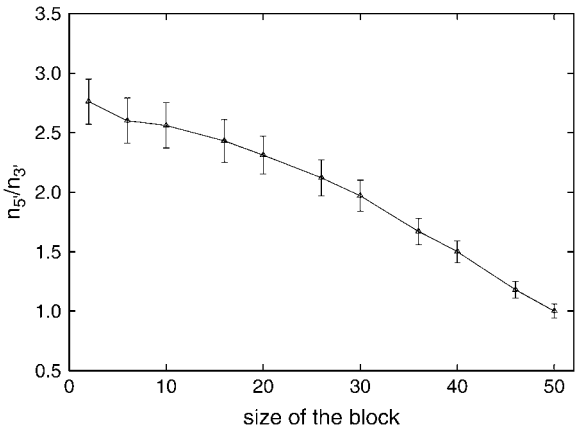

FIGURE 9 Dependence of bias on the size of a biotin-streptavidin block centered on the DNA. The system is otherwise the same as in Figs. 2 and 3.

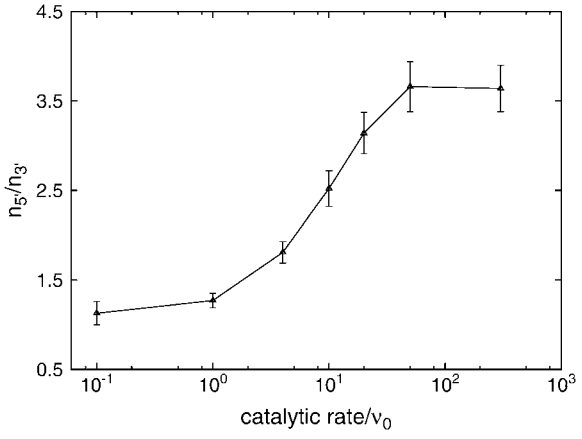

FIGURE 8 Influence of finite catalytic rate (imperfect sink at the reaction site) on preferential repair. The system is otherwise the same as in Figs. 2 and 3.

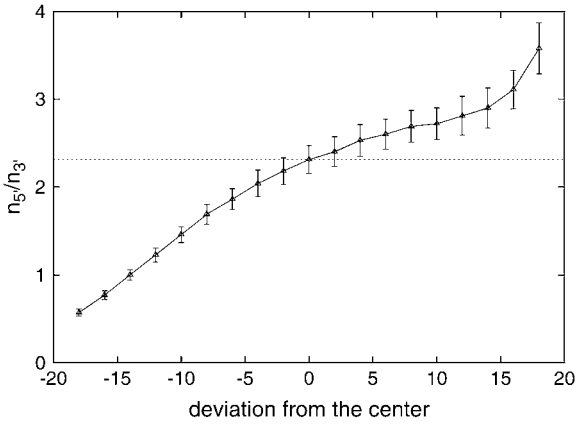

FIGURE 10 Dependence of the bias on the position of the block. In the simulations presented, the block has a constant size of 20 nt. The point ''0'' on the horizontal axis corresponds to the point at which the center of the block coincides with that of the DNA, and the dashed line denotes the bias at this particular position.

only ~15 lattice spacings, which we expect to correspond to ~75 nt based on the size of an AGT molecule. This persistence length results from the fact that protein copies must unbind at a finite rate to maintain microscopic reversibility in this thermally driven system. At most, we find a 5′:3′ repair ratio of ~10, and it is achieved in the limit of high DNA occupancy. Determining whether this requirement is likely to be met in vivo requires better quantitation of copy numbers and salt effects in cellular environments.

We thank Norbert Scherer, Yihan Lin, Xing Jian, and Chuan He for helpful discussions and critical readings of the manuscript.

The work was supported by a Multi-University Research Initiative grant from the Army Research Office and National Science Foundation CAREER Award MCB-0547854.

REFERENCES

1. Riggs, A. D., S. Bourgeois, and M. Cohn. 1970. The *lac* repressor-operator interaction. III. Kinetic studies. *J. Mol. Biol.* 53:401–417.
2. von Hippel, P. H., and O. G. Berg. 1989. Facilitated target location in biological systems. *J. Biol. Chem.* 264:675–678.
3. Adam, G., and M. Delbruck. 1968. Reduction in dimensionality in biological diffusion processes. *In* Structural Chemistry and Molecular Biology. W. H. Freeman and Co., New York. 198–215.
4. Berg, O. G., R. B. Winter, and P. H. von Hippel. 1981. Diffusion-driven mechanisms of protein translocation on nucleic acids. 1. Models and theory. *Biochemistry.* 20:6929–6948.
5. Shimamoto, N. 1999. One-dimensional diffusion of proteins along DNA. *J. Biol. Chem.* 274:15293–15296.
6. Slutsky, M., and L. A. Mirny. 2004. Kinetics of protein-DNA interaction: facilitated target location in sequence-dependent potential. *Biophys. J.* 87:4021–4035.
7. Halford, S. E., and J. F. Marko. 2004. How do site-specific DNA-binding proteins find their target? *Nucleic Acids Res.* 32:3040–3052.
8. Sokolov, I. M., R. Metzler, K. Pant, and M. C. Williams. 2005. Target search of *N* sliding proteins on a DNA. *Biophys. J.* 89:895–902.
9. Alberts, B., A. Johnson, J. Lewis, M. Raff, K. Roberts, and P. Walter. 2002. Molecular Biology of the Cell, 4th Ed. Garland Science, New York.
10. Howard, J. 2001. Mechanics of Motor Proteins and the Cytoskeleton. Sinauer Associates, New York.
11. Daniels, D. S., T. T. Woo, K. X. Luu, D. M. Noll, N. D. Clarke, A. E. Pegg, and J. A. Tainer. 2004. DNA binding and nucleotide flipping by the human DNA repair protein AGT. *Nat. Struct. Mol. Biol.* 11:714–720.
12. Begley, T. J., and L. D. Samson. 2004. Reversing DNA damage with a directional bias. *Nat. Struct. Mol. Biol.* 11:688–690.
13. Rasimas, J. J., A. E. Pegg, and M. G. Fried. 2003. DNA-binding mechanism of O^6-alkylguanine-DNA alkyltransferase. *J. Biol. Chem.* 278:7973–7980.
14. Rasimas, J. J., S. R. Kar, A. E. Pegg, and M. G. Fried. 2007. Interactions of human O^6-alkylguanine-DNA alkyltransferase (AGT) with short single-stranded DNAs. *J. Biol. Chem.* 282:3357–3366.
15. Bortz, A. B., M. H. Kalos, and J. L. Lebowitz. 1975. A new algorithm for Monte Carlo simulation of Ising spin systems. *J. Comput. Phys.* 17:10–18.
16. Gillespie, D. T. 1977. Exact stochastic simulation of coupled chemical reactions. *J. Phys. Chem.* 81:2340–2361.
17. Newman, M. E. J., and G. T. Barkema. 1999. Monte Carlo Methods in Statisical Physics. Clarendon Press, Oxford, UK.
18. Blainey, P. C., A. M. van Oijen, A. Banerjee, G. L. Verdine, and X. S. Xie. 2006. A base-excision DNA-repair protein finds intrahelical lesion bases by fast sliding in contact with DNA. *Proc. Natl. Acad. Sci. USA.* 103:5752–5757.
19. Schurr, J. M. 1979. The one-dimensional diffusion coefficient of proteins absorbed on DNA. Hydrodynamic considerations. *Biophys. Chem.* 9:413–414.
20. Zang, H., Q. Fang, A. E. Pegg, and F. P. Guengerich. 2005. Kinetic analysis of steps in the repair of damaged DNA by human O^6-alkylguanine-DNA alkyltransferase. *J. Biol. Chem.* 280:30873–30881.